Suppression of the dynamic transition in surface water at low hydration levels: A study of water on rutile

Eugene Mamontov
Neutron Scattering Science Division, Oak Ridge National Laboratory, Oak Ridge, Tennessee 37831, USA

Lukas Vlcek
Department of Chemical Engineering, Vanderbilt University, Nashville, Tennessee 37235, USA

David J. Wesolowski
Chemical Sciences Division, Oak Ridge National Laboratory, Oak Ridge, Tennessee 37831, USA

Peter T. Cummings
Department of Chemical Engineering, Vanderbilt University, Nashville, Tennessee 37235-1604, USA
and Center for Nanophase Materials Sciences, Oak Ridge National Laboratory, Oak Ridge, Tennessee 37831, USA

Jörgen Rosenqvist
Chemical Sciences Division, Oak Ridge National Laboratory, Oak Ridge, Tennessee 37831, USA

Wei Wang
Environmental Sciences Division, Oak Ridge National Laboratory, Oak Ridge, Tennessee 37831, USA

David R. Cole and Lawrence M. Anovitz
Chemical Sciences Division, Oak Ridge National Laboratory, Oak Ridge, Tennessee 37831, USA

Goran Gasparovic
NIST Center for Neutron Research, Gaithersburg, Maryland 20899, USA
and Department of Materials Science and Engineering, University of Maryland, College Park, Maryland 20742, USA
(Received 8 December 2008; revised manuscript received 6 March 2009; published 22 May 2009)

Our quasielastic neutron-scattering experiments and molecular-dynamics simulations probing surface water on rutile (TiO_2) have demonstrated that a sufficiently high hydration level is a prerequisite for the temperature-dependent crossover in the nanosecond dynamics of hydration water. Below the monolayer coverage of *mobile* surface water, a weak temperature dependence of the relaxation times with no apparent crossover is observed. We associate the dynamic crossover with interlayer jumps of the mobile water molecules, which become possible only at a sufficiently high hydration level.

DOI: 10.1103/PhysRevE.79.051504 PACS number(s): 61.20.Lc, 61.05.fj, 61.20.Ja

The origin of a dynamic crossover in water, recently observed in quasielastic neutron-scattering (QENS) experiments [1–3] and initially attributed to the "fragile"-to-"strong" liquid transition, has been extensively debated [4–13]. In the temperature range of 210–230 K, the relaxation times obtained from QENS measurements show a crossover between high-temperature non-Arrhenius and low-temperature Arrhenius behavior. QENS experiments have found the crossover in water in various environments, such as carbon nanotubes [14,15] and confined aqueous solutions [16], as well as in water adsorbed onto oxide surfaces [17–19]. Observation of the crossover in hydration water in lysozyme [20], DNA [21], and RNA [22] has sparked even more heated debate concerning the role of hydration water in the apparent dynamic transition in biomolecules, which coincides with the onset of their bioactivity, especially because other studies found no evidence of the crossover around 225 K [23]. While some studies question the relationship between the dynamics of hydration water and the host biomolecules [24,25], or even the existence of a well-defined dynamic transition in biomolecules [26,27], majority agree that the dynamic properties of the host biomolecules are influenced by the hydration water [8,28–30] (see Doster [31] for a recent discussion). One view is that water acts as a plasticizer modulating the barriers of the energy landscape that controls the dynamics of the biomolecules. However, some studies go even further to suggest, based on the similarity of the transition temperatures, that the dynamic transition in hydration water triggers the dynamic transition in the host biomolecules [12,13,20–22].

We have analyzed the hydration level dependence of the dynamic transition in water sorbed on rutile (TiO_2) nanoparticle surfaces using data from QENS experiments and molecular-dynamics (MD) simulations. We report that the dynamic transition in surface water, measurable on the time scale of hundreds of picoseconds, is suppressed as the hydration level is decreased, and is no longer detectable when less than one monolayer of mobile water is present on the surface. In the presence of more than a monolayer of mobile water, the transition is related to the layer-exchange jumps, thus representing only a limited subset of diffusion dynamics

in hydration water. Therefore, the temperature-dependent dynamic transition in surface water (at least on simple oxide surfaces) may be merely a signature of sufficiently high water coverage or hydration level.

Rutile nanopowders with a predominant (110) surface face and a surface area of 180–183 m^2/g were synthesized as described elsewhere [18]. Following cleaning by repeated dialysis in deionized water and drying in vacuum at 333 K, the dry powders were loaded into aluminum sample holders [18] and placed in a vacuum oven enclosed within a glove bag. The samples were then evacuated at 413 K after which the glove bag was purged and flooded with ultrapure argon passed through a cryotrap. After venting the oven with this dry atmosphere, premeasured aliquots of water were added to each sample using a precalibrated micropipette. The sample holders were then quickly sealed, placed back in the oven, and held at 333 K overnight to ensure equilibration with water. Because evacuation at 413 K does not remove all water from the nanoparticle surface [18], the total water amounts sorbed on the samples were determined from a linear correlation ($r^2=0.995$) observed between the elastic neutron-scattering intensities measured at 5 K versus the added water mass. From these results, we conclude that the samples in the QENS experiment had absolute hydration levels of 1.52, 2.50, and 3.50 H_2O molecules per Ti_2O_4 surface unit. In terms of surface layers, L_1, L_2, and L_3, defined as water molecules located between the minima of the MD axial density profile of water oxygen atoms near the (110) surface [18], these correspond to $(L_1+0.5L_2)$, $(L_1+L_2+0.3L_3)$, and $(L_1+L_2+L_3)$. The first hydration level, L_1, consists predominantly of molecular H_2O (rather than hydroxyl groups, OH) chemisorbed atop five-coordinated Ti atoms exposed on the surfaces. The molecules of L_1 are essentially immobile (except for some very limited localized motions) on the time scale of the QENS experiment [18,19]. Thus, the samples that we studied had (1) half a layer, (2) a layer and a third, and (3) two layers of mobile water. The L_1 layer is not readily removable by means of outgassing even at elevated temperatures [32] and can be considered an intrinsic part of the TiO_2 surface. In this sense, the hydration level reported as monolayer coverage in nonoxide systems such as biomolecules may be comparable with the (L_1+L_2) coverage on TiO_2 surface; two monolayer coverage in biomolecules may be comparable with the $(L_1+L_2+L_3)$ coverage on TiO_2 surface, etc.

The QENS experiments were carried out at the high-flux backscattering spectrometer (HFBS) [33] at the NIST Center for Neutron Research (NCNR) operated with a dynamic range of ± 11 μeV and energy resolution of 0.8 μeV (full width at half maximum). The sample loading and the experimental setup were the same as described before [18]. Integrating the data over the range of energy transfers, $0.62\ \text{Å}^{-1} < Q < 1.60\ \text{Å}^{-1}$ (at the elastic channel), was possible because of the very weak Q dependence of the QENS broadening due to the spatially restricted character of the molecular motions [18,19]. The QENS data presented in Fig. 1 were fit with the following expression:

$$S(E) = \left[x\delta(E) + (1-x)\left(p\frac{1}{\pi}\frac{\Gamma_1}{E^2+\Gamma_1^2} + (1-p)\frac{1}{\pi}\frac{\Gamma_2}{E^2+\Gamma_2^2} \right) + (C_1 + C_2 E) \right] \otimes R(E). \quad (1)$$

The term in square brackets, convolved with the resolution function $R(E)$ (the latter is represented by the 5 K fully elastic scattering data from the corresponding sample), includes the elastic signal centered at zero-energy transfer, two Lorentzian components and a linear background term that accounts for the dynamics which are too fast on the time scale of the experiment. The elastic signal originates from the weak scattering by rutile, scattering from immobile species such as the L_1 molecules, and may also include a contribution due to spatial restriction of the motions that give rise to the QENS broadening. Due to a very limited dynamic range of the HFBS experiment of ± 11 μeV, only the narrow Lorentzian component with a half-width at half maximum (HWHM) of Γ_1 can be determined reliably. The broader Lorentzian component due to faster relaxations cannot be measured reliably on the HFBS; however, its inclusion improves the quality of the fits. Due to the weakness of the QENS signal, we could use only one Lorentzian component plus a linear background for the fits of the sample with the lowest hydration level. The relaxation times for the diffusion component reliably accessible on the HFBS are shown in Fig. 2.

In the $(L_1+L_2+L_3)$ data, there is a pronounced dynamic crossover at 217 K between the high-temperature Vogel-Fulcher-Tammann (VFT) behavior, $\tau(T) = \tau_0 \exp[DT_0/(T-T_0)]$ (here the dimensionless parameter D is not related to the diffusion coefficient), and the low-temperature Arrhenius behavior, $\tau(T) = \tau_0 \exp(E_a/RT)$, where $\tau_0=419$ ps, $D=0.06$, $T_0=207$ K, and $E_a=2.4$ kJ/mol. In the $(L_1+L_2+0.3L_3)$ data, the crossover is much less pronounced, but still can be detected at 228 K with $\tau_0=392$ ps, $D=0.14$, $T_0=199$ K, and $E_a=1.8$ kJ/mol. Finally, the $(L_1+0.5L_2)$ data exhibit a nearly temperature-independent relaxation time of about 600 ps.

The MD simulations assessed the behavior of water on the (110) surface of rutile, at temperatures and surface hydration levels identical to experimental conditions, except for the temperature point of 200 K, which would require the longest computation time. As in our previous studies [18,19], water was represented by the simple point charge/extended model and the surface water interaction parameters were obtained from an *ab initio* force field described by Bandura *et al.* [34,35]. The repeating simulation cell consisted of water molecules adsorbed on two parallel rutile blocks 40 Å apart with a total of 144 Ti_2O_4 surface (110) units. Long-range interactions were calculated using the Ewald summation with a two-dimensional correction [36]. For different hydration levels and temperatures, the simulations span the times of 50–200 ns. Figure 3 shows the relaxation times for the slower component obtained from the MD data fits with two Debye components over the dynamic range corresponding to the QENS experiment.

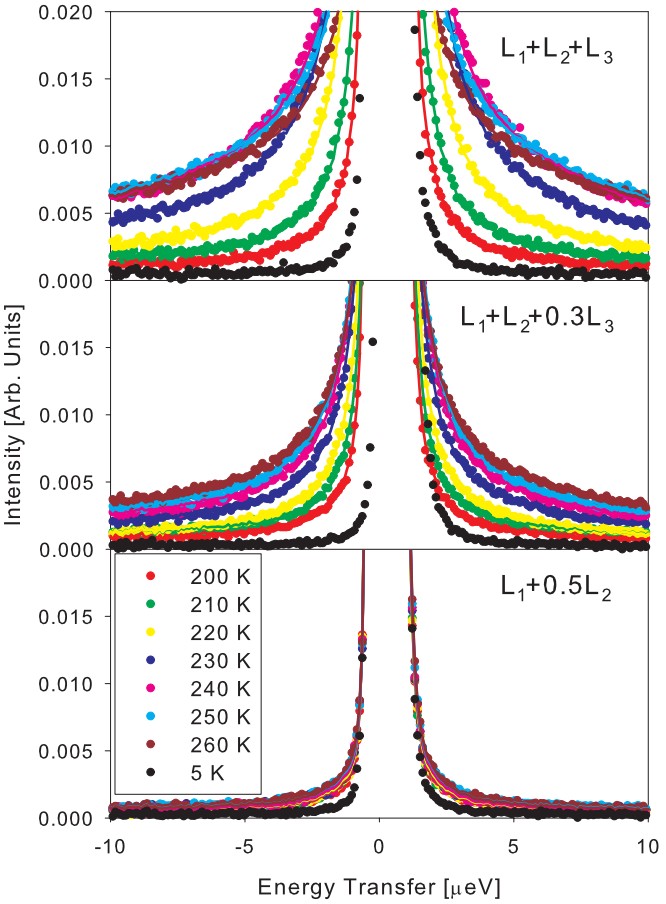

FIG. 1. (Color) QENS data (symbols) and fits (solid lines) with Eq. (1) (single Lorentzian fit for the lowest hydration level).

It is immediately obvious that, while there are differences in the absolute values of the characteristic relaxation times, compared with the values extracted from the QENS experiment shown in Fig. 2, qualitatively, the same behavior is observed for each hydration level. In the $(L_1+L_2+L_3)$ data, the dynamic crossover can be seen at 240 K between the high-temperature VFT fit, $\tau(T)=\tau_0 \exp[DT_0/(T-T_0)]$ and the low-temperature Arrhenius fit, $\tau(T)=\tau_0 \exp(E_a/RT)$, where $\tau_0=320$ ps, $D=0.2$, $T_0=206$ K, and $E_a=2.4$ kJ/mol. In the $(L_1+L_2+0.3L_3)$ data, the dynamic crossover can be seen at 237 K, with the parameters $\tau_0=186$ ps, $D=0.4$, $T_0=197$ K, and $E_a=3.9$ kJ/mol. Even though it is possible to fit the data in a different manner, for instance, by selecting four instead of three points for the VFT fits, we have found that only the fits shown in Fig. 3 could yield the same value of the parameter τ_0 for the VFT and Arrhenius fits, which was a constraint that we imposed. Finally, the $(L_1+0.5L_2)$ data can be reasonably represented by a temperature-independent relaxation time of about 1322 ps. At this lowest hydration level, both the QENS and MD relaxation times show little temperature dependence, but the QENS relaxation times are shorter by a factor of 2 compared to the MD relaxation times. This is not unexpected in view of the fact that QENS data for the $(L_1+0.5L_2)$ coverage could be fit with only one Lorentzian component plus a linear background, whereas the fits of the MD data, free of the experimental

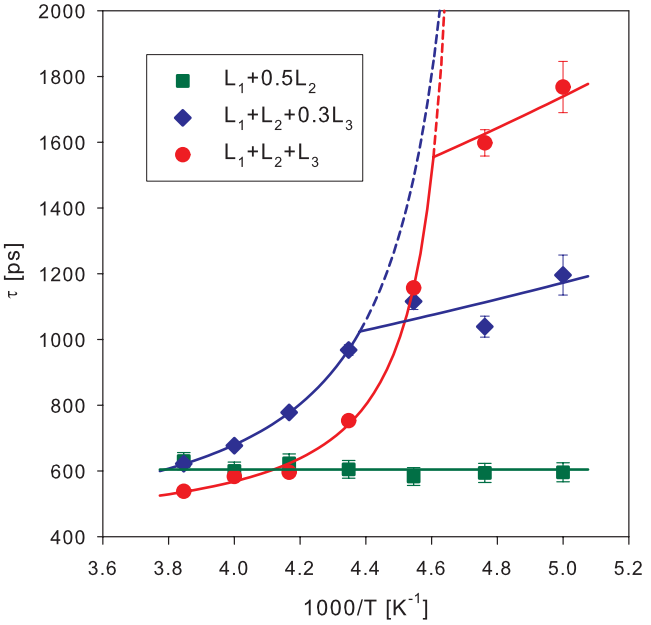

FIG. 2. (Color) The characteristic relaxation times calculated from the HWHM (Γ_1) of the narrow (or, for the lowest hydration level, the only) Lorentzian component of the QENS data fits as $\tau=\hbar/\Gamma_1$. Also shown are fits with VFT, Arrhenius, and temperature-independent functions.

background, required two components. Most significantly, both the QENS and MD data show that at low hydration (below one monolayer coverage of the mobile surface water), the temperature-dependent dynamic crossover can no longer be observed and is replaced by the set of relaxation times with little temperature dependence.

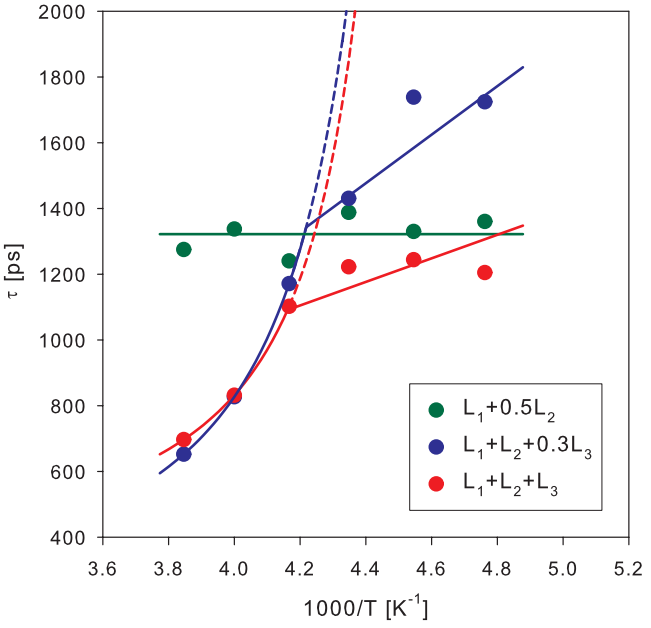

FIG. 3. (Color) The relaxation times for the slower component obtained from the MD data fits with two Debye components. Also shown are fits of the relaxation times with VFT, Arrhenius, and temperature-independent functions.

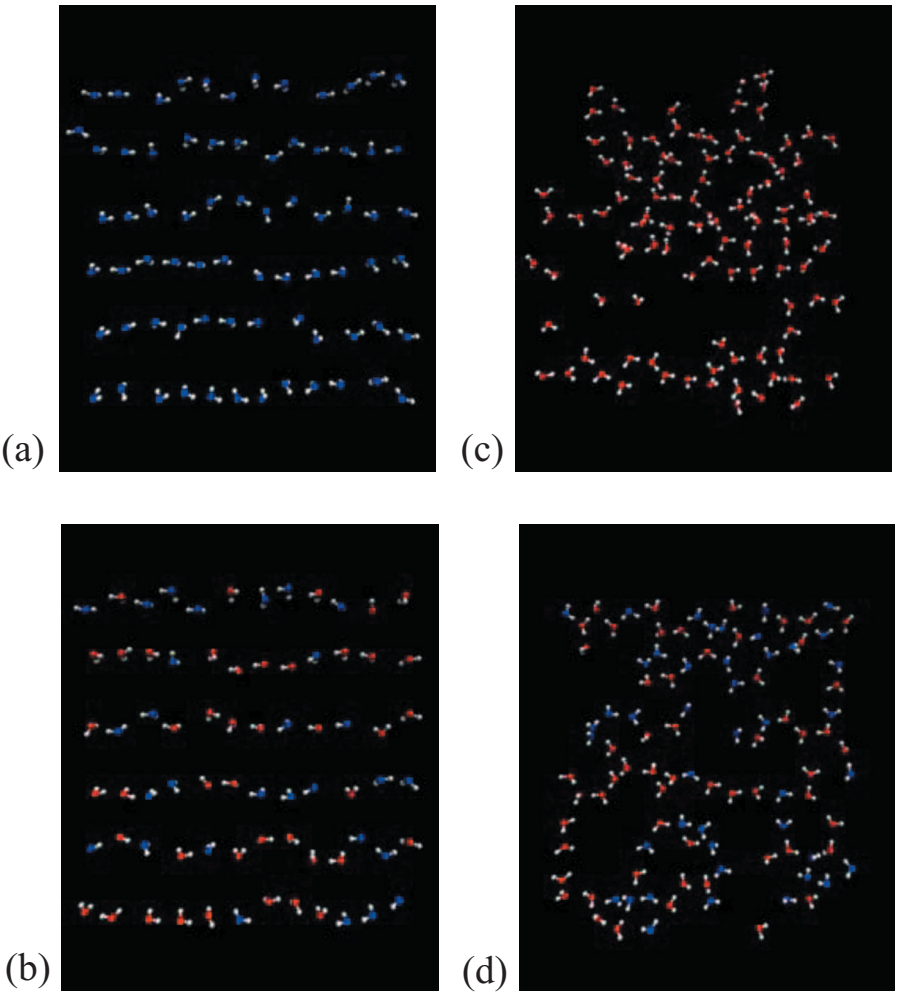

FIG. 4. (Color) Snapshots of the simulation data [planar views perpendicular to the (110) rutile surface, only L_2 and L_3 layers are shown for clarity] for the highest hydration level at 260 K, at $t=0$ (after MD equilibration) and $t=1000$ ps. The oxygen atoms of the water molecules that were residing in the L_2 and L_3 layers at $t=0$ are shown in blue and red, respectively. Top left (a): L_2 at $t=0$ ps. Bottom left (b): L_2 at $t=1000$ ps. Top right (c): L_3 at $t=0$ ps. Bottom right (d): L_3 at $t=1000$ ps.

Figure 4 shows representative MD snapshots of the water structure and demonstrates the important fact that the dynamic component on the time scale of hundreds of picoseconds associated with the dynamic transition observed in surface water originates from interlayer jumps [19]. Over a time period of 1000 ps, a molecule has a reasonable probability of interlayer exchange through a process with a characteristic time of hundreds of picoseconds. Molecules residing in the L_2 layer at any given time exhibit a suppressed lateral (but not rotational) mobility. For this reason, one can readily observe the fraction of layer-exchanging molecules by means of comparing the top and bottom snapshots on the left; the "red" molecules that originated in the L_3 layer at $t=0$ and subsequently jumped into the L_2 layer do not change their lateral positions, just their orientations. On the other hand, the "blue" molecules that originated in the L_2 layer at $t=0$ and subsequently jumped into the L_3 layer participate in lateral translational motion, as one can see on the snapshots shown on the right. Importantly, both the localized rotational (in the L_2 and L_3) and the lateral translational motions (in the L_3 only) take place on the time scale of picoseconds and tens of picoseconds and are much faster compared to the layer-exchange jumps [19]. Indeed, over a period of 1000 ps, each water molecule makes a number of reorientational and translational (for the L_3 layer) jumps. These diffusion components yield the QENS signal contributing to the faster component in the HFBS experiment, which is too broad for the HFBS dynamic range to be assessed reliably. It is the narrower component in both the HFBS experiments and the MD simulations (associated with the layer-exchange jumps) that exhibits the dynamic transition. In the absence of water molecules in the L_3 layer (low hydration levels), the interlayer jumps are no longer possible; thus, there is no dynamic crossover. Below monolayer coverage of mobile water, the dynamics on the time scale of hundreds of picoseconds originates from different types of motions that involve "lone" molecules of the L_2 layer. Both the QENS and MD data for the $(L_1+0.5L_2)$ sample actually show a rather unusual trend for the relaxation times, which can be described as either temperature independent or even saddlelike, with a shallow minimum in the midtemperature range. Similar behavior has been previously observed by dielectric spectroscopy for confined water [37–41]. In one study the saddlelike behavior was attributed to the loss of hydration water at higher temperatures [41]. The explanation proposed in the other studies was that the minimum in the relaxation times resulted from competition between the activation energy, which favors faster dynamics at higher temperatures, and the increasing free volume effects, which favor faster dynamics at lower temperatures [38–40]. This interpretation is applicable to our low-coverage data given the fact that a lone water molecule occupies a larger "free volume" compared to a water mol-

ecule belonging to a cluster of L_2 molecules. This is because the former makes hydrogen bonds with two bridging oxygen atoms, thus occupying twice as much space as a water molecule associated with the clusters.

We would like to draw an important analogy between the dynamic components in hydration and bulk (or confined) water. We have previously found [19] three distinct dynamic components for hydration water. The fastest one originates from the motions of the outermost water molecules which, on average, do not form four hydrogen bonds. This component has no analogy in bulk or confined water. The intermediate dynamic component is due to rotationlike localized motions of all water molecules. This component is analogous to the "rotational" diffusion component in bulk of confined water. Such motions are thermally activated and exhibit Arrhenius temperature dependence. The slowest dynamic component in hydration water is associated with the interlayer jumps. It is analogous to "translational" diffusion component in bulk or confined water in that they require simultaneous breaking of several hydrogen bonds. Thus, they both exhibit non-Arrhenius dependence at higher temperatures and a dynamic crossover.

It should be noted that a dielectric spectroscopy study of supercooled water confined in a vermiculite clay [42] reported that one of the relaxation processes (the slowest and the strongest of all the processes observed) was conditioned upon the presence of two layers of water molecules in the clay interlayer space. This process was attributed to the dynamics of the water molecules not in direct contact with the clay walls. Thus, this process may be qualitatively similar to the slow relaxation process in the surface water that we discuss in the present work in a sense that they both may involve interlayer exchange of water molecules. Obviously, the presence of more than one layer of mobile water is a prerequisite for such interlayer exchange.

In summary, both the QENS and MD data demonstrate disappearance (at submonolayer coverage of mobile water) of the dynamic crossover as the hydration level is decreased. This is consistent with assignment of the dynamics that gives rise to the crossover behavior to layer-exchange motions, which cannot start until the water coverage exceeds one monolayer. On the one hand, our results may seem to be in agreement with the hypothesis that the dynamic transition in hydration water triggers the dynamic transition in host biomolecules. This is because of the well-known fact that the dynamic transition in biomolecules does not take place at low hydration level; only at approximately monolayer water coverage and above, the dynamics of biomolecules become qualitatively similar to those observed at full hydration [43,44]. Similarly, we find that the dynamic transition in surface water develops immediately above one layer coverage of mobile water. On the other hand, it seems more plausible that there is no direct cause and effect relationship between the dynamic transitions in the hydration water and the hydrated host biomolecules. Instead, it is the increasing amount of hydration water that eventually makes both transitions possible. The transition in hydration water becomes possible due to the appearance of water molecules on top of one mobile layer, which enables interlayer exchange. The increasing water clustering and eventual formation of a full hydrogen-bonded network due to percolation effects that promotes a plasticizing influence on the biomolecule dynamics [45] provides adequate explanation of the dynamic transition in the host biomolecules. This holds true whether the dynamic transition is due to a sudden change in the biomolecules dynamics or merely represents the entrance of the smoothly increasing amplitude of the biomolecules motions into the resolution window of the experiment [26,27]. The common prerequisite for both types of dynamic transitions, in the hydration water and the hydrated biomolecules, is the sufficient amount of hydration water.

Note added in proof. After this paper has been accepted, we have measured the dynamics of hydration water on forsterite, Mg_2SiO_4, using a different neutron backscattering spectrometer (BASIS at the Spallation Neutron Source, Oak Ridge National Laboratory). Interestingly, the dependence of the relaxation times on the hydration level was qualitatively very similar to that shown in Fig. 2 of this paper. In particular, the crossover at the intermediate hydration level was shifted to a higher temperature compared to the crossover at the high hydration level. This suggests that the dependence of the crossover position on the hydration level presented in Fig. 2 may be rather universal, at least for the systems with hydrophilic surface-water interactions. Furthermore, the dynamical crossover in hydrated tRNA recently measured by Roh *et al.* [46] also shows a shift to higher temperatures as the hydration level is decreased.

ACKNOWLEDGMENTS

The authors are thankful to K. W. Herwig and M. Zamponi for critical reading of the paper. We used the resource of the Computing Center for Research and Education at Vanderbilt University and the Institutional Computational Cluster at ORNL's Chemical Sciences Division. This work was supported by the U.S. DOE, BES, Division of Chemical Sciences, Geosciences, and Biosciences through the project "Nanoscale Complexity at the Oxide/Water Interface" (Project No. ERKCC41) and by Oak Ridge National Laboratory, managed by UT-Battelle, LLC, for the U.S. DOE under Contract No. DE-AC05-00OR22725.

[1] A. Faraone, L. Liu, C.-Y. Mou, C.-W. Yen, and S.-H. Chen, J. Chem. Phys. **121**, 10843 (2004).

[2] L. Liu, S.-H. Chen, A. Faraone, C.-W. Yen, and C.-Y. Mou, Phys. Rev. Lett. **95**, 117802 (2005).

[3] L. Liu, S.-H. Chen, A. Faraone, C.-W. Yen, C.-Y. Mou, A. I. Kolesnikov, E. Mamontov, and J. Leao, J. Phys.: Condens. Matter **18**, S2261 (2006).

[4] J. Swenson, Phys. Rev. Lett. **97**, 189801 (2006); S. Cerveny,

J. Colmenero, and A. Alegria, *ibid.* **97**, 189802 (2006); S. H. Chen, L. Liu, and A. Faraone, *ibid.* **97**, 189803 (2006).
[5] S. Cerveny, J. Colmenero, and A. Alegria, Eur. Phys. J. Spec. Top. **141**, 49 (2007).
[6] J. Hedstrom, J. Swenson, R. Bergman, H. Jansson, and S. Kittaka, Eur. Phys. J. Spec. Top. **141**, 53 (2007).
[7] N. Bjerrum, Science **115**, 385 (1952).
[8] J. Swenson, H. Jansson, J. Hedstrom, and R. Bergman, J. Phys.: Condens. Matter **19**, 205109 (2007).
[9] D. E. Moilanen, N. E. Levinger, D. B. Spry, and M. D. Fayer, J. Am. Chem. Soc. **129**, 14311 (2007).
[10] V. Garbuio, C. Andreani, S. Imberti, A. Pietropaolo, G. F. Reiter, R. Senesi, and M. A. Ricci, J. Chem. Phys. **127**, 154501 (2007).
[11] L. Xu, P. Kumar, S. V. Buldyrev, S.-H. Chen, P. H. Poole, F. Sciortino, and H. E. Stanley, Proc. Natl. Acad. Sci. U.S.A. **102**, 16558 (2005).
[12] P. Kumar, Z. Yan, L. Xu, M. G. Mazza, S. V. Buldyrev, S.-H. Chen, S. Sastry, and H. E. Stanley, Phys. Rev. Lett. **97**, 177802 (2006).
[13] M. Lagi, X.-Q. Chu, C. Kim, F. Mallamace, P. Baglioni, and S.-H. Chen, J. Phys. Chem. B **112**, 1571 (2008).
[14] E. Mamontov, C. J. Burnham, S.-H. Chen, A. P. Moravsky, C.-K. Loong, N. R. de Souza, and A. I. Kolesnikov, J. Chem. Phys. **124**, 194703 (2006).
[15] X.-Q. Chu, A. I. Kolesnikov, A. P. Moravsky, V. Garcia-Sakai, and S.-H. Chen, Phys. Rev. E **76**, 021505 (2007).
[16] E. Mamontov, D. R. Cole, S. Dai, M. D. Pawel, C. D. Liang, T. Jenkins, G. Gasparovic, and E. Kintzel, Chem. Phys. **352**, 117 (2008).
[17] E. Mamontov, J. Chem. Phys. **123**, 171101 (2005).
[18] E. Mamontov, L. Vlcek, D. J. Wesolowski, P. T. Cummings, W. Wang, L. M. Anovitz, J. Rosenqvist, C. M. Brown, and V. Garcia-Sakai, J. Phys. Chem. C **111**, 4328 (2007).
[19] E. Mamontov, D. J. Wesolowski, L. Vlcek, P. T. Cummings, J. Rosenqvist, W. Wang, and D. R. Cole, J. Phys. Chem. C **112**, 12334 (2008).
[20] S.-H. Chen, L. Liu, E. Fratini, P. Baglioni, A. Faraone, and E. Mamontov, Proc. Natl. Acad. Sci. U.S.A. **103**, 9012 (2006).
[21] S.-H. Chen, L. Liu, X.-Q. Chu, Y. Zhang, E. Fratini, P. Baglioni, A. Faraone, and E. Mamontov, J. Chem. Phys. **125**, 171103 (2006).
[22] X.-Q. Chu, E. Fratini, P. Baglioni, A. Faraone, and S.-H. Chen, Phys. Rev. E **77**, 011908 (2008).
[23] M. Vogel, Phys. Rev. Lett. **101**, 225701 (2008).
[24] K. Wood, M. Plazanet, F. Gabel, B. Kessler, D. Oesterhelt, D. J. Tobias, G. Zaccai, and M. Weik, Proc. Natl. Acad. Sci. U.S.A. **104**, 18049 (2007).
[25] K. Wood, M. Plazanet, F. Gabel, B. Kessler, D. Oesterhelt, G. Zaccai, and M. Weik, Eur. Biophys. J. **37**, 619 (2008).
[26] A. P. Sokolov, J. H. Roh, E. Mamontov, and V. Garcia-Sakai, Chem. Phys. **345**, 212 (2008).
[27] S. Khodadadi, S. Pawlus, J. H. Roh, V. Garcia-Sakai, E. Mamontov, and A. P. Sokolov, J. Chem. Phys. **128**, 195106 (2008).
[28] A. M. Tsai, D. A. Neumann, and L. N. Bell, Biophys. J. **79**, 2728 (2000).
[29] M. Tarek and D. J. Tobias, Phys. Rev. Lett. **88**, 138101 (2002).
[30] A. L. Tournier, J. Xu, and J. C. Smith, Biophys. J. **85**, 1871 (2003).
[31] W. Doster, Eur. Biophys. J. **37**, 591 (2008).
[32] J. Boerio-Goates, G. Li, L. Li, T. F. Walker, T. Parry, and B. F. Woodfield, Nano Lett. **6**, 750 (2006).
[33] A. Meyer, R. M. Dimeo, P. M. Gehring, and D. A. Neumann, Rev. Sci. Instrum. **74**, 2759 (2003).
[34] H. J. Berendsen, J. R. Grigera, and T. P. Straatsma, J. Phys. Chem. **91**, 6269 (1987).
[35] A. V. Bandura and J. D. Kubicki, J. Phys. Chem. B **107**, 11072 (2003).
[36] I.-C. Yeh and M. L. Berkowitz, J. Chem. Phys. **111**, 3155 (1999).
[37] A. Gutina, E. Axelrod, A. Puzenko, E. Rysiakiewicz-Pasek, N. Kozlovich, and Y. Feldman, J. Non-Cryst. Solids **235-237**, 302 (1998).
[38] Y. Ryabov, A. Gutina, V. Arkhipov, and Y. Feldman, J. Phys. Chem. B **105**, 1845 (2001).
[39] L. Frunza, H. Kosslick, S. Frunza, and A. Schonhals, J. Phys. Chem. B **106**, 9191 (2002).
[40] L. Frunza, H. Kosslick, I. Pitsch, S. Frunza, and A. Schonhals, J. Phys. Chem. B **109**, 9154 (2005).
[41] J. Sjöström, J. Swenson, R. Bergman, and S. Kittaka, J. Chem. Phys. **128**, 154503 (2008).
[42] R. Bergman, J. Swenson, L. Borjesson, and P. Jacobsson, J. Chem. Phys. **113**, 357 (2000).
[43] P.-H. Yang and J. A. Rupley, Biochemistry **18**, 2654 (1979).
[44] J. A. Rupley and G. Careri, Adv. Protein Chem. **41**, 37 (1991).
[45] A. Oleinikova, N. Smolin, and I. Brovchenko, Biophys. J. **93**, 2986 (2007) and references therein.
[46] J. Roh, R. Briber, A. Damjanovic, D. Thirumalai, S. Woodson, and A. Sokolov, Biophys. J. **96**, 2755 (2009).